

GALACTIC HALO STELLAR STRUCTURES IN THE TRIANGULUM-ANDROMEDA REGION*

NICOLAS F. MARTIN

Max-Planck Institut für Astronomie, Königstuhl 17, D-69117 Heidelberg, Germany

RODRIGO A. IBATA

Observatoire de Strasbourg, 11 rue de l'Université, F-67000 Strasbourg, France

AND

MIKE J. IRWIN

Institute of Astronomy, Madingley Road, Cambridge CB3 0HA, U.-K.

Draft version March 21, 2007

ABSTRACT

This letter reports on the Galactic stellar structures that appear in the foreground of our Canada-France-Hawaii-Telescope/MegaCam survey of the halo of the Andromeda galaxy. We recover the main sequence and main sequence turn-off of the Triangulum-Andromeda structure recently found by Majewski and collaborators at a heliocentric distance of ~ 20 kpc. The survey also reveals another less populated main sequence at fainter magnitudes that could correspond to a more distant stellar structure at ~ 28 kpc. Both main sequences are smoothly distributed over the $\sim 54\text{deg}^2$ covered by the survey but they show a density increase toward the Galactic plane that does not appear to be due to contamination from the Galactic disk or stellar halo. The discovery of a stellar structure behind the Triangulum-Andromeda structure that itself appears behind the low-latitude stream that surrounds the Galactic disk gives further evidence that the inner halo of the Milky Way is of a spatially clumpy nature.

Subject headings: Galaxy: evolution — Galaxy: halo — Galaxy: structure — Local Group

1. INTRODUCTION

The stellar halos of galaxies such as our own Milky Way are expected to have formed over time by the accretion of stellar material from satellites falling within its gravitational potential (e.g. Freeman & Bland-Hawthorn 2002 and references therein). The discovery of the disrupting Sagittarius dwarf galaxy (Ibata, Gilmore & Irwin 1994) and the stream of stars it leaves in the Galactic halo (Ibata et al. 2001a, 2002; Majewski et al. 2003) has revealed that such accretions indeed take place at the present time. Currently, the best evidence for the clumpy nature of the inner halo of the Milky Way ($D \lesssim 50$ kpc) is given by the Sloan Digital Sky Survey (SDSS) whose mapping of the North Galactic Cap by Belokurov et al. (2006) shows numerous coherent streams or more fuzzy and diffuse stellar structures believed to be remnants of past accretions.

Aside from large sky surveys such as the SDSS, the search for stellar structures surrounding the Milky Way has also strongly benefited from wide-field mappings of the Andromeda galaxy (M31) and its neighborhood. These mainly photometric surveys need to be deep enough to track M31 red giant branch (RGB) stars and therefore also contain the brighter and bluer main se-

quence stars that belong to foreground stellar structures. Ibata et al. (2003) have used their Isaac Newton Telescope (INT) survey to show that the low latitude stream (LLS) that surrounds the Milky Way disk is present towards M31. Kinematics of these main sequence stars also agree with previous detections of this stream, on a roughly circular orbit around our Galaxy (Martin et al. 2006a). Using ten deeper fields observed within $\sim 10^\circ$ from M31, Majewski et al. (2004) have revealed that another stellar structure can be seen behind the low-latitude stream as a fainter main sequence. A companion paper by Rocha-Pinto et al. (2004) tracks this so-called Triangulum-Andromeda structure with RGB stars selected in the 2MASS catalogue. Spectroscopic follow-up of these stars unveiled a metallicity $[\text{Fe}/\text{H}] \sim -1.2$ and a low velocity dispersion consistent with an accretion origin.

In this paper, we take advantage of our deep and wide survey of the Southern quadrant of the M31 outer halo to study these foreground stellar structures. The survey was observed with the MegaCam wide-field camera mounted on the Canada-France-Hawaii Telescope and currently represents the deepest wide dataset towards M31. We use it to characterize the Triangulum-Andromeda (TriAnd) structure and reveal yet another main sequence fainter than TriAnd and that could correspond to a farther stellar structure. § 2 briefly presents the dataset while § 3 studies the two main sequences that appear in the color-magnitude diagram of the MegaCam data. § 4 concludes this letter.

2. DATA

The extent of the MegaCam survey is delimited in Figure 1 (double-line polygon) and corresponds to

*BASED ON OBSERVATIONS OBTAINED WITH MEGAPRIME/MEGACAM, A JOINT PROJECT OF CFHT AND CEA/DAPNIA, AT THE CANADA-FRANCE-HAWAII TELESCOPE (CFHT) WHICH IS OPERATED BY THE NATIONAL RESEARCH COUNCIL (NRC) OF CANADA, THE INSTITUT NATIONAL DES SCIENCES DE L'UNIVERS OF THE CENTRE NATIONAL DE LA RECHERCHE SCIENTIFIQUE (CNRS) OF FRANCE, AND THE UNIVERSITY OF HAWAII.

Electronic address: martin@mpia-hd.mpg.de

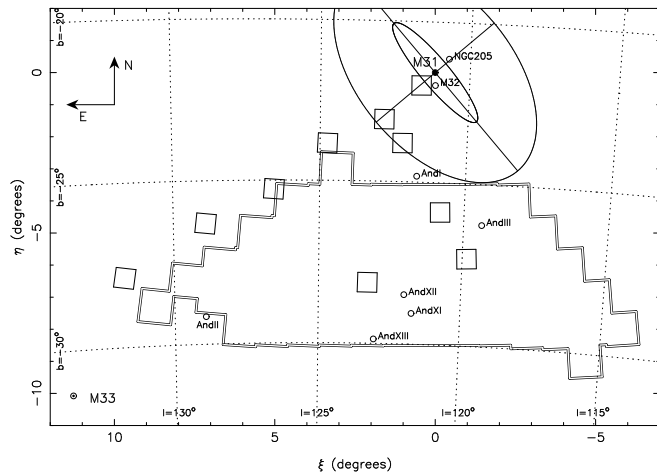


FIG. 1.— Extent of the MegaCam survey in the southern quadrant of the M31 halo (double line). North is to the top and East to the left. The dotted line corresponds to a grid in Galactic coordinates. M31 is at the center of the Figure and known M31 satellites are represented by circles or a dotted circle in the case of M33. The inner ellipse around M31 approximately corresponds to its HI disk with a radius of 27 kpc while the outer ellipse marks a distance of 50 kpc and ellipticity 0.6. The INT survey (Ibata et al. 2003) in which the TriAnd structure is observed fills the outer ellipse. The ten fields that Majewski et al. (2004) used to discover the structure are shown as squares.

60 MegaCam fields covering ~ 54 sq. deg. observed between 2003–2006. Compared to Martin et al. (2006b), three fields that lie close to the M33 galaxy are not considered here. They contain young M33 stars that contaminate the blue regions of the color-magnitude diagram where foreground Galactic MS are found. Figure 1 also shows the location of the fields that were used by Majewski et al. (2004) to discover TriAnd.

Due to length constraints, we refer the reader to Ibata et al. (2007) for details on the observing and reduction of the MegaCam survey.

3. RESULTS

The Hess diagram of the $\sim 1.3 \times 10^6$ stars found in the MegaCam survey is shown Figure 2. The most obvious feature is produced by red-giant branch (RGB) stars at the distance of the Andromeda galaxy at $i_0 \gtrsim 21.0$ and $(g-i)_0 \gtrsim 0.5$. The broadness of this feature is due to the numerous structures with different metallicities that are traced in the halo of M31. These include metal-poor dwarf galaxies such as And II and III that create the bluer RGBs and the Ibata et al. (2001) metal-rich giant stream that is currently disrupting in the M31 halo and produces the redder RGBs (see Ibata et al. 2007 for more details on these structures related to the Andromeda galaxy). Foreground Galactic disk dwarf stars at various distances along the line of sight create the red feature at $(g-i)_0 \sim 2.0$ and populate the CMD in the $i_0 \lesssim 20.0$ region as these stars evolve along their main sequence. Finally, the TriAnd main sequence (MS) turn-off clearly appears in the bluer regions of the CMD and extends from $(g-i, i)_0 \sim (0.3, 19.5)$ down to $(g-i, i)_0 \sim (0.8, 22.5)$. This main sequence “forks” at $i_0 \sim 21.5$ to reveal another more diffuse main sequence at fainter magnitudes. This fainter MS has to our knowledge never been detected before probably due to its faintness (for instance, the INT survey of the inner halo of M31 in which LLS and TriAnd

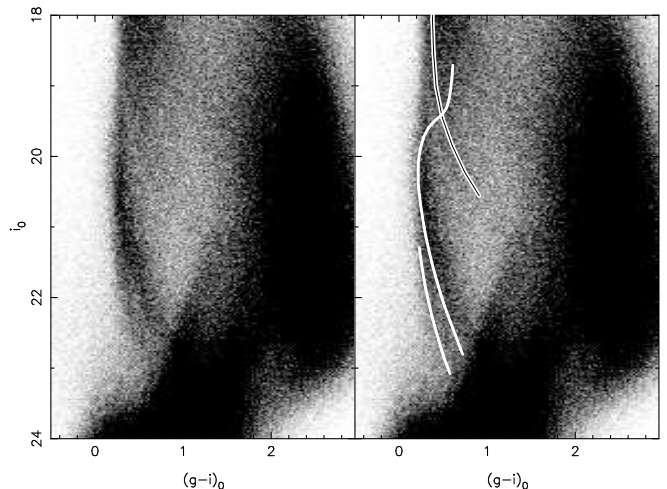


FIG. 2.— Hess diagram of the $\sim 1.3 \times 10^6$ stars in the MegaCam survey. The densest features at the bottom of the diagram and in the $(g-i)_0 \gtrsim 2.0$ region correspond to background M31 and foreground Milky Way disk stars respectively. The main sequence of the TriAnd structure is clearly visible between $(g-i, i)_0 \sim (0.3, 19.5)$ and $(g-i, i)_0 \sim (0.8, 22.5)$. Another fainter and more diffuse main sequence is also visible for $i_0 \gtrsim 21.5$ before it merges with the TriAnd MS. On the right panel, the double line corresponds to the LLS main sequence as detected by Ibata et al. (2003) and the white lines represent the Girardi et al. (2004) isochrone of 10 Gyr and $[\text{Fe}/\text{H}] \sim -1.3$ shifted to a distance modulus of 16.5 and 17.25 to adjust the TriAnd and TriAnd2 MS, respectively.

are detected is not deep enough to show it) and its low density that prevent detections from deep “pencil-beam” observations toward M31.

The ridge of the LLS main sequence discovered by Ibata et al. (2003) in their INT survey has been plotted in the right panel of Figure 2. No such main sequence appears in the MegaCam survey but this is not unexpected since the density of the LLS MS drops exponentially with Galactic latitude and has almost disappeared at $b \sim -24^\circ$ in the INT fields which are still North of the MegaCam survey. The TriAnd MS is ~ 2 magnitudes fainter than the LLS fiducials but the bluer turn-off of TriAnd ($(g-i)_0 \sim 0.15$) compared to LLS ($(g-i)_0 \sim 0.4$) probably indicates a difference in age and/or metallicity between the two structures and therefore precludes a simple shift of the LLS fiducial to determine the distance to TriAnd. However, using the spectroscopic metallicity measured for TriAnd RGB stars ($[\text{Fe}/\text{H}] \sim -1.2$; Rocha-Pinto et al. 2004), one can constrain the age and distance of the structure from the color and magnitude of the turn-off. It can be seen on the right panel of Figure 2 that the Girardi et al. (2004) isochrone with a metallicity $Z = 0.001$ (corresponding to $[\text{Fe}/\text{H}] \sim -1.3$), an age of 10 Gyr and a distance modulus of 16.5 gives a good agreement with the MegaCam observations. This corresponds to a heliocentric distance of ~ 20 kpc and a Galactocentric distance of ~ 25 kpc. Although the turn-off of the fainter MS is hidden behind the TriAnd MS and MS turn-off, the same isochrone provides a good fit when assuming a distance modulus of 17.25. This converts to heliocentric and Galactocentric distances of ~ 28 kpc and ~ 33 kpc respectively. For clarity, we will call this new feature TriAnd2 hereafter.

Figure 3 shows the evolution of the two MSs as a func-

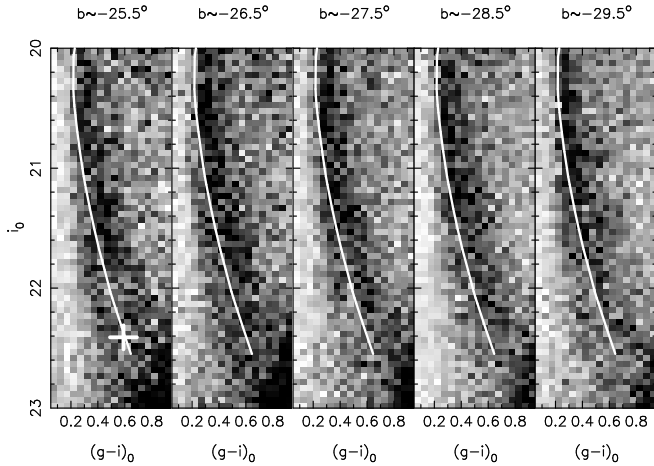


FIG. 3.— Evolution of the MSs with Galactic latitude. In each diagram, the counts have been normalized to a the same area and the isochrone that fits the blue edge of the TriAnd MS in Figure 2 has been reproduced. The cross in the left panel corresponds to the location of the MS in the Majewski et al. (2004) fields that overlap with the MegaCam survey.

tion of the declination strip observed with MegaCam. It can be seen on Figure 1 that these strips almost exactly correspond to 1-degree wide strips in Galactic latitude between $b \sim -25^\circ$ and $b \sim -30^\circ$. The Hess diagrams of Figure 3 were normalized to the number of fields in each strip, between 9 for the Northern-most strip and 13 for the Southern-most one. This difference in the number of fields propagates into the noise of the diagrams and the one at $b \sim -29.5^\circ$ appears less noisy than the one at $b \sim -25.5^\circ$. Nevertheless, the diagrams show no significant change in distance with Galactic latitude since the isochrone always provides a good match to the blue ridge of the TriAnd MS (the TriAnd2 MS has a lower density that makes it very difficult to follow in the Hess diagrams of Figure 3 that only cover $\sim 10\text{deg}^2$). Neither does a similar analysis along the Galactic longitude direction unveil any sign of distance gradient. Taken at face value, this is at variance with the findings of Majewski et al. (2004), who reported a ~ 0.37 magnitude shift in distance modulus (or $\sim 19\%$ in distance) between their three Northern-most fields (those that are within the outer ellipse of Figure 1) and their three Southern-most fields (the three fields that are within the MegaCam survey). However their estimate of the blue edge of the MS in their Southern-most fields is represented by the white cross in the left panel of Figure 3 and it matches the MegaCam data well¹. It is therefore possible that the TriAnd structure gets closer in regions to the North of the survey but this distance gradient does not extend to the MegaCam survey itself: the structure would then not be smooth over the sky.

Both main sequences have their density diminish with Galactic latitude. This is hinted at by the diagrams of Figure 3 where the MSs seem to have lower densities from left to right and is confirmed by Figure 4 that traces the evolution of the density of the two MSs (bottom and central panels) in the selection boxes reported on the right

¹ To convert magnitudes in the Washington ($M, M - T_2$) system to the MegaCam ($i, g - i$), we first use Majewski et al. (2004) transformations to the ($i', V - i'$) system and then the Ibata et al. (2007) transformation to the MegaCam magnitudes.

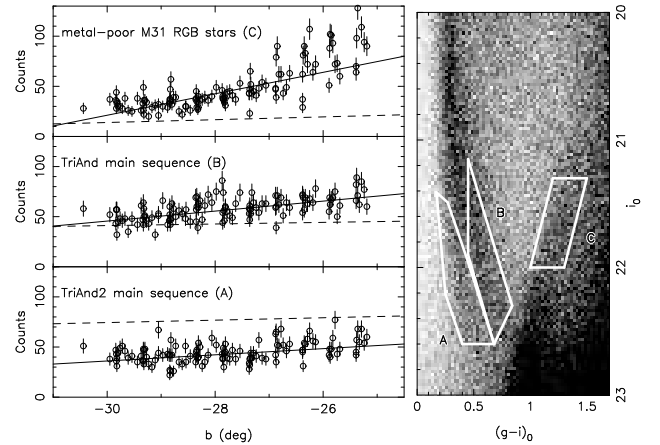


FIG. 4.— Density evolution of the TriAnd2 (bottom panel) and TriAnd (middle panel) stellar structures as well as the metal-poor M31 RGB stars (top panel) with Galactic latitude. In all cases the star-counts correspond to the number of stars in each selection box within a half MegaCam field ($\sim 0.45\text{deg}^2$). A linear slope has been fitted to the data in the three panels and provides a good fit to the MW stellar structures but not to the M31 structures. The density is determined from the selection boxes shown over the Hess diagram on the right panel with box A selecting TriAnd2 MS stars, box B TriAnd MS stars and box C M31 metal-poor RGB stars.

panel Hess diagram. The TriAnd selection box (labeled B) has been purposely cut at a redder limit than the MS turn-off to avoid the region where the TriAnd2 MS merges with the TriAnd MS. A selection box (C) has also been placed on the metal-poor RGB of M31-related stellar structures for comparison since the faint end of the MSs could be contaminated by these distant M31 stars.

Both MSs show a constant increase in their density with increasing Galactic latitude² that is well matched by a simple linear slope. On the contrary, the metal-poor M31 RGB stars more closely resemble an exponential increase with latitude (top panel of Figure 4). Moreover, the density of this population shows a significant scatter in the Northern region of the MegaCam survey ($b \gtrsim -27^\circ$). This is expected since these fields are closer to M31 and probe M31-related stellar structures whose density vary from field to field (see Ibata et al. 2007). The absence of this scatter and the exponential rise in the TriAnd and TriAnd2 MSs density panels make it unlikely that selection boxes A and B are contaminated by M31-related stars. Moreover, the absence of a strong scatter around the best linear fits shows the smoothness of the two structures on the sky that do not show any central concentration in the MegaCam data.

Since there is no field in the MegaCam survey that does not contain the MS features, there is no easy way to eliminate the possibility that the increasing density with latitude observed in Figure 4 is not due to an underlying Galactic population (disk or smooth halo). The presence of M31 stars to the red of the selection boxes also prevents a simple estimation of the contaminants from regions of the Hess diagram surrounding the boxes. However at brighter magnitudes ($21.0 < i_0 < 22.0$) the merged MSs stand out clearly in the Hess diagram and such an estimation can be performed. For each strip of MegaCam fields that were used to produce Figure 3, a

² A similar analysis in Galactic longitude shows no trend of the density of the MSs in this direction.

third order polynomial is fit at the same time to regions bluer and redder than the MS to estimate the Galactic contamination under the MSs. The fit is then subtracted from the star counts in the merged MS to yield an increase from ~ 170 to ~ 270 stars per MegaCam field over the 5° of Galactic latitude covered by the survey. This increase is higher than the $\sim 30\%$ increase of the combined linear fits of the two MSs in Figure 4 and confirms that if selection boxes A and B indeed contain contaminants, these tend to lower and not steepen the Galactic latitude density gradient of the two structures. The density of the two MSs observed in Figure 4 therefore seem to be real and not linked to Galactic contaminants.

The Besançon model (Robin et al. 2003) can also provide another verification that these MSs are not related to smooth Galactic components (in particular the stellar halo). The linear fits found in the selection boxes for the simulated region $120^\circ < \ell < 125^\circ$ and $-30^\circ < b < -25^\circ$ are shown as thin dashed lines in the left panels of Figure 4 (the counts have also been normalized to half a MegaCam field to allow a direct comparison). The higher model star counts in selection box A compared to the observed star counts could indicate that the stellar halo component that is used in the model (and that is not well constrained; see Robin, Reylé & Crézé 2000) is not adequate for the region towards M31. Nevertheless, these fits show increases of only a few percents for both MSs and are different from the slopes fitted to the MegaCam data. Moreover, no turn-off is observed in the color-magnitude diagram of the model as stars belonging to the stellar halo form a straight blue edge at $(g-i)_0 \sim 0.2$ and never bend to redder colors as the MSs do in Figure 2. Interestingly, a comparison of the COSMOS data with the Besançon model reveals that a “hook-like” feature very similar to the MSs observed towards M31 is probably due to a stellar structure that inhabits the Milky Way halo in this direction (Robin et al. 2007). Therefore, the TriAnd2 MS does not seem to be linked to a smooth Galactic components (disk or smooth stellar halo) and is more likely a stellar structure that inhabits the inner halo of the Milky Way.

Finally, assuming the MSs are produced by stellar structures in the Milky Way halo, we can measure the surface brightness Σ_V of the combined MS in the region of the CMD where the Galactic contamination can be measured ($21.0 < i_0 < 22.0$). Assuming that all the stars belong to the closer TriAnd MS, this will give a bright limit to the TriAnd surface brightness. The magnitude ranges corresponds to $4.7 < M_V < 5.8$ and represents 16% of the luminosity of the stellar population when using the luminosity function from Silvestri et al. (1998) with an age of 10 Gyr, $Z = 0.001$ and a mass function as m^{-2} . This mass function gives the lowest contribution to the upper main sequence for all the lu-

minosity functions they propose and will therefore give a bright limit to Σ_V . This leads to $\Sigma_V = 32.5 \text{ mag/arcsec}^2$ over the whole MegaCam survey, in reasonable agreement with the bright limits measured in the same way by Majewski et al. (2004; $\Sigma_V = 32.1$ or 32.4 depending on their isochrone assumptions). However, it does not take into account the merging of the two MSs in the region of the CMD that was used. For instance, if 25% of the stars in fact belong to the fainter TriAnd2 main sequence, the surface brightness of TriAnd would be only $\sim 32.8 \text{ mag/arcsec}^2$.

4. DISCUSSION

The presence of two Galactic stellar structures in the MegaCam data at Galactocentric distances of ~ 25 and $\sim 33 \text{ kpc}$, added to the low-latitude stream observed only a few degrees away (Ibata et al. 2003) shows the clumpy nature of the inner halo of the Milky Way in this region. But since these structures do not show any boundary within the $\sim 54 \text{ deg}^2$ covered here, there is no reason that this conclusion should only be applied toward M31. In fact, each step forward in the depth and/or coverage of the inner halo reveals hitherto undetected stellar structures within a few tens of kiloparsecs (e.g. Belokurov et al. 2006, Robin et al. 2007). This increasingly clumpy nature of the inner halo of the Galaxy is reminiscent of the inner halo of M31 which also contains many structures on circular orbits out to $\sim 50 \text{ kpc}$ (Ibata et al. 2005).

However, this does not rule out that some of these stellar structures could be linked together. It has already been proposed by Majewski et al. (2004) that the TriAnd structure could be another loop of the low latitude stream, produced by its progenitor spiraling towards the Galactic center. Simulations of the stream by Peñarrubia et al. (2005) or Martin et al. (2005) indeed show that TriAnd is a natural outcome of such an accretion. Could the new structure found here also be related to TriAnd? The good fit of the same isochrone to both main sequences in Figure 2 indicates a similar stellar population. However, the turn-off of this structure is bluer than that of the low-latitude stream and would argue against a link with it although it could also indicate that the putative progenitor of all these structures contained a stellar population gradient. A definite answer will have to wait for spectroscopic observations of the new structure to determine from their radial velocities if they are on orbits compatible with TriAnd and the low-latitude stream.

We are grateful to the CFHT staff for performing the MegaCam observations in queue mode.

Facilities: CFHT (MegaCam).

REFERENCES

- Belokurov V. et al., 2006, ApJ 642, L137
- Freemna K. & Bland-Hawthorn J., 2002, ARA&A 40, 487
- Girardi L., Grebel E. K., Odenkirchen M. & Choisi C., 2004, A&A 422, 205
- Ibata R. A., Gilmore G. & Irwin M. J., 1994, Nature 370, 194
- Ibata R., Lewis G., Irwin M., Totten E. & Quinn T., 2001a, ApJ 551, 294
- Ibata R. A., Irwin M. J., Lewis G. F., Ferguson A. M. N. & Tanvir N. R., 2001, Nature 412, 49
- Ibata R., Lewis G., Irwin M. & Cambrésy L., 2002, MNRAS 332, 921
- Ibata R. A., Irwin M. J., Lewis G. F., Ferguson A. M. N. & Tanvir N. R., 2003, MNRAS 340, L21
- Ibata R., Chapman S., Ferguson A. M. N., Lewis G. F., Irwin M. J. & Tanvir N. R., 2005, ApJ 634, 287
- Ibata R. A., Martin N. F., Irwin M. J., Chapman S. C., Ferguson A. M. N. & Lewis G. F., 2007, MNRAS submitted

- Majewski S. R., Skrutskie M. F., Weinberg M. D., Ostheimer J. C., 2003, *ApJ* 599, 1082
- Majewski S. R., Ostheimer J. C., Rocha-Pinto H. J., Patterson R. J., Guhathakurta P. & Reitzel D., 2004, *ApJ* 615, 738
- Martin N. F., Ibata R. A., Conn B. C., Lewis G. F., Bellazzini M. & Irwin M. J., 2005, *MNRAS* 362, 906
- Martin N. F., Irwin M. J., Ibata R. A., Conn B. C., Lewis G. F., Bellazzini M., Chapman S. C. & Tanvir N. R., 2006a, *MNRAS* 367, L69
- Martin N. F., Ibata R. A., Irwin M. J., Chapman S. C., Lewis G. F., Ferguson A. M. N. & Tanvir N. R., 2006b, *MNRAS* 371, 1983
- Peñarrubia J. et al., 2005, *ApJ* 626, 128
- Robin A. C., Reylé C. & Cr     M., 2000, *A&A* 359, 103
- Robin A. C., Reyl     C., Derri     & Picaud S., 2003, *A&A* 409, 523
- Robin A. C. et al., 2007, *ApJS* accepted, astro-ph/0612349
- Rocha-Pinto H. J., Majewski S., Skrutskie M. F., Crane J. D. & Patterson R. J., 2004, *ApJ* 615, 732
- Silvestri F., Ventura P., D'Antona F. & Mazzitelli I., 1998, *ApJ* 509, 192